16TH EUROPEAN CONFERENCE ON EARTHQUAKE ENGINEERING
THESSALONIKI 18 - 21 JUNE 2018

DAMAGE INDEX FOR STRUCTURES WITH ELEMENTS OF HIGH FLEXURAL STIFFNESS AND/OR BRITTLE BEHAVIOR

Diego HIDALGO-LEIVA[1], Luis PUJADES[2], Alex BARBAT[3], Sergio DIAZ[4], Yeudy VARGAS-ALZATE[5], Luis A. PINZÓN[6]

ABSTRACT

Structures with high lateral stiffness and/or with brittle to semi-brittle elements in their lateral resistant system may exhibit a rapid decrease of their shear capacity and a sudden loss of stiffness when lateral cyclic loads, as those produced by earthquakes, are applied. This behavior can be related to damage (partial or complete) of a particular structural element. In this article, the expected seismic damage is analyzed and assessed in two different structures. The first one is a low-rise reinforced masonry structure, with hollow concrete blocks (2 stories); the second one is a high-rise dual reinforced concrete building (18 stories). In both cases, materials are characterized using a proper hysteresis model, which takes into account softening and shear degradation. To quantify the structural damage, the well-known Park and Ang damage index is used. The damage curves shown in this paper, exhibit a quick damage increase for relatively low-intensity values, which is attributed to nonlinear incursions of several structural elements with low ultimate ductility. However, incremental dynamic analyses are time-consuming; therefore, it becomes important to develop simplified methods, also successfully representing this kind of effects. A recently proposed damage index, which can be computed in an easy and straightforward way from capacity curves or capacity spectra, is modified in this work to include this fast strength degradation. Details of the computations of this new damage index are also described here.

Keywords: Damage; Brittle; Ductile, Stiffness Degradation

1. INTRODUCTION

Structural damage due to seismic actions, and for any particular action, is the result of a combination of a large number of variables, which can be interpreted and simplified by means of “easy to understand” models. Mostly, damage models were initially proposed to describe the observed damage in regular frame structures, with both reinforced concrete and structural steel. One of the most implemented damage index is the Park and Ang (1985) Damage Index (DI_{PA}). It was fitted for ductile damage in 142 monotonically loaded reinforced concrete beams and columns. The first index uses a combination of two different damage sources: displacement ductility and hysteretic energy.

For ductile structures, like those with special moment frames, and for small inelastic deformations, the ratio between the ductility demand at that point and the ultimate ductility factor, contributes little to the damage index. On the contrary, if the structure is composed of low ductility elements, small ductility demands, may produce a stronger increase of the damage index This differences in the structural behavior are thus responsible for significant differences in the shape of the damage index curves and, therefore, on the expected damage.

[1]Ph.D., Civil Engineering School, University of Costa Rica, San José, Costa Rica, diego.hidalgo@ucr.ac.cr
[2]Ph.D., DECA, Technical University of Catalonia, Barcelona, Spain, lluis.pujades@upc.edu
[3]Ph.D., DECA, Technical University of Catalonia, Barcelona, Spain, alex.barbat@upc.edu
[4]Ph.D., DAIA, Autonomic University Juárez of Tabasco, Tabasco, Mexico, sergio.alberto.diaz@upc.edu
[5]Ph.D., DECA, Technical University of Catalonia, Barcelona, Spain, yeudy.felipe.vargas@upc.edu
[6]M.Sc., DECA, Technical University of Catalonia, Barcelona, Spain, luis.pinzon@upc.edu

In this work, nonlinear incremental static and dynamic analyses are performed in two different structures. The expected damage is analyzed by means of the DI_{PA} obtained with Incremental Dynamic Analysis (IDA). Then the obtained DI_{PA} is compared with a simplified capacity-curve-based damage index (Pujades et al. 2015), which can be obtained from the pushover curve in a simple and straightforward way. Also, a modification of this simplified damage index is proposed, in order to take into account, the differences in the damaging pattern of low and high ductility systems.

2. CASE OF STUDY

Two structural models are used to quantify damage in their structural elements. Both models were implemented in RUAUMOKO 3D (Carr 2003) software, carrying out nonlinear static and dynamic analyses.

2.1 Reinforced Concrete Masonry (RCM) structure

A Costa Rican typical dwelling is used herein for the characterization the RCM typology. This is a low-rise two-stories building with a shear predominant behavior, which was designed and constructed according to the Costa Rican Seismic Code 2010 (CSCR-10) (CFIA 2011). Walls distribution and stories height correspond to a real structure which was designed and inspected by the first author of this paper, and is considered representative for this typology. The masonry compression design resistance was set at f'_m=100 kg/cm^2.

The distribution of walls is shown in Figure 1. In all the cases, hollow concrete blocks with 12cm of thickness were used. The walls distribution of the second floor is the same as the one of the first floor with the exception that walls W-3 and W-4 in Figure 1, are not used. An equivalent frame model is used in Ruaumoko3D software (Carr 2003). The elements are modelled as Giberson (1967) beam-columns elements, with perfect plastic hinges on the base of the wall and a rigid beam on the upper section. Several authors have used this solution for similar models (D'Ayala et al. 2014; Kingsley et al. 2014; Lagomarsino et al. 2013; Madan et al. 1997; Seible et al. 1994). The beam element placed in the top of the walls has elastic properties and high stiffness, so it can be considered as a rigid beam. In the sections between walls, a regular elastic beam is used with the aim of concentrate the damage on the walls. A full detail of the hysteretic curve employed to model the walls behavior can be found in Hidalgo-Leiva et al. (2016) and Hidalgo-Leiva (2017).

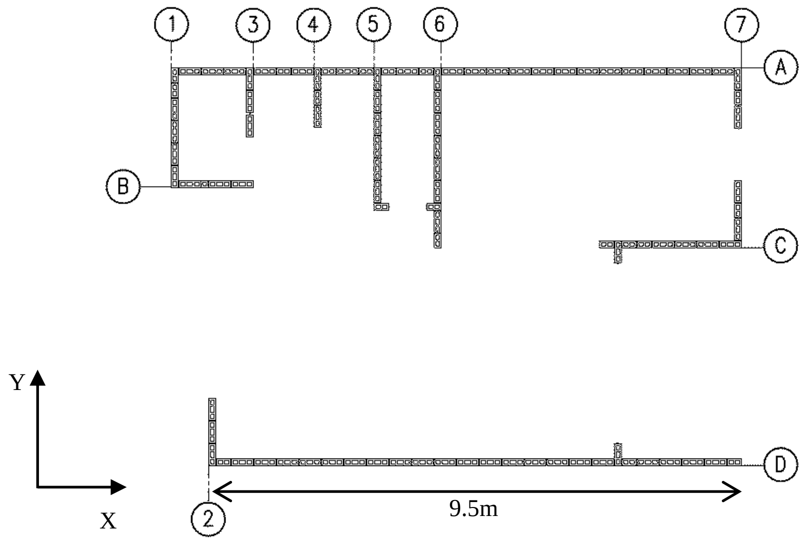

Figure 1. Walls distribution on the first floor of the RCM structure.

A lumped mass model was used in the modal analysis. The dead load takes the weight of the structure, architectural finishes and electro-mechanical elements. The live load is set as 2.5 kN/m^2 on the first level and 0.5 kN/m^2 for the roof diaphragm, according to CSCR-10 for residential use (CFIA 2011). The lumped mass of the first and second levels are 78.32 kN s^2/m and 38.1 kN s^2/m respectively. A rigid diaphragm is defined for both levels. The height between levels is 2.75 m. The period of the first mode of vibration is 0.27 s in the Y direction and 0.12 s in the X direction with a mass participation factor of 92% in both cases.

For structural design purposes, the CSCR-10 (CFIA 2011) defines a PGA equal to 0.36 g for soil class S_3 (that is equivalent to soil class D in ASCE 7-16 (ASCE 2017)) and seismic zone III, which covers the capital city and its surroundings. This PGA is used for a deterministic evaluation of the performance of these structures.

2.2 Dual Reinforced Concrete (DRC) structure

The DRC structure which has been studied is a regular residential building with 18 stories, above the ground, with a dual system of reinforced concrete with a compression design resistance equal to f'_c= 350 kg/cm^2. Figure 2 shows the distribution of the vertical elements that are part of the lateral load resistance system. It is composed by 2 square columns (RC-1:80x80cm and RC-2:60x60cm) and three rectangular walls (MC-1:40x195cm, MC-2:40x275cm and MC-3:60x600cm). Detailing and design were performed according to the CSCR-10 (CFIA 2011) and ACI 318-08 (2008).

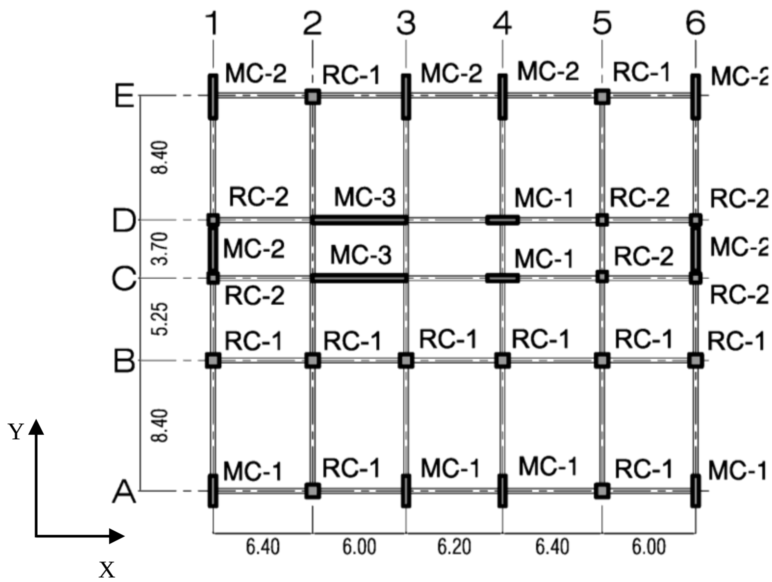

Figure 2. Plan view of the vertical structural elements distribution for the DRC structure.

For the nonlinear description, the Revised Takeda model (Carr 2003) is used with the parameters shown in Table 1, where α is the positive Bilinear factor, β is the negative Bilinear factor, γ is the unloading power factor, δ is the reloading intersection factor, φ is the ratio of compression to tensile stiffness, FCRP is the Cracking action as ratio of positive yield, FCRN is the cracking action as ratio of negative yield.

Table 1. Required parameters to fully define the Revised Takeda hysteresis model (Carr 2003).

α	β	γ	δ	φ	FCRP	FCRN
0.9	0.9	0.0	0.0	1.0	0.8	0.8

These values were defined according to the recommendation of the Ruaumoko 3D manual (Carr 2003) and the parametric study of Esquivel (1992). In addition to this flexural plastic hinge, a SINA hysteresis curve (Saidi and Sozen 1979) was used to model the shear degradation in shear walls. The SINA model is defined by the parameters shown in Table 2, where $\boldsymbol{\alpha}$ is the positive Bilinear factor, $\boldsymbol{\beta}$ is the negative Bilinear factor, $\boldsymbol{F_{cr}}$ is the Cracking moment or force and $\boldsymbol{F_{cc}}$ is the Crack closing moment or force. A more detailed definition of the structure and the hysteresis models employed can be found in Hidalgo-Leiva (2017).

Table 2. Required parameters to define SINA hysteresis model (Carr 2003).

$\boldsymbol{\alpha}$	$\boldsymbol{\beta}$	$\boldsymbol{F_{cr}}$	$\boldsymbol{F_{cc}}$
0.5	0.5	0.85	0.65

From a modal analysis, the first mode period in X direction is 2.16 s with a mass participation factor of 0.75 and 2.31 seconds with a mass participation factor of 0.73 in the Y direction. The PGA selected in the design procedure was 0.36 g, same as for the previous case, due to the geographical location of the main cities in Costa Rica.

3. THE SEISMIC ACTION

Two different evaluations of the nonlinear behavior are performed. The first one corresponds to an incremental static load or Pushover analysis, taking the first deformation mode as the load pattern. The second one is the Incremental Dynamic Analysis (IDA) defined by Vamvatsikos and Cornell (2002). This analysis implies the application of a seismic action in the form of an acceleration record with different amplitude values, evaluating the differences in the response when the amplitude of the seismic action increases.

According to CSCR-10, for nonlinear dynamic analysis, a set of 3 different accelerograms must be used in order to compute the mean response of the structure. For the RCM structure, the 1991 Limon earthquake (Mw 7.7) recorded in Cartago city (CCTG) (Jacob and Pacheco 1991), the 2001 El Salvador earthquake (Mw 7.7) recorded in la Libertad station (ESLI) (Bommer et al. 2010) and the 2012 Samara earthquake (Mw 7.6) recorded in Samara station (GNSR) (Linkimer et al. 2013) were used; meanwhile, for the DRC structure the Limon earthquake is replaced by the 2009 Cinchona earthquake (Mw 6.2) recorded in Alajuela station (CINCH) (RSN 2009). This change is due to the minimum frequency employed in the passband filter for the CCTG record, which is 0.8 Hz, so it becomes a record not suitable for the analysis of structures with natural periods above 1.2 seconds.

With the aim of constraining the dispersion of the structural response, all the records were treated with spectral matching (Hancock and Bommer 2007), defining a period observation window according with the ASCE 7-16 (ASCE 2017). The target response spectrum was defined according to the CSCR-10 (CFIA 2011). The intensity measure used as scale factor was the PGA, having different ranges of values in order to reach the structural collapse. Figure 3 shows the spectrally matched response spectra for both structures, comparing them with the target spectrum (CSCR-10).

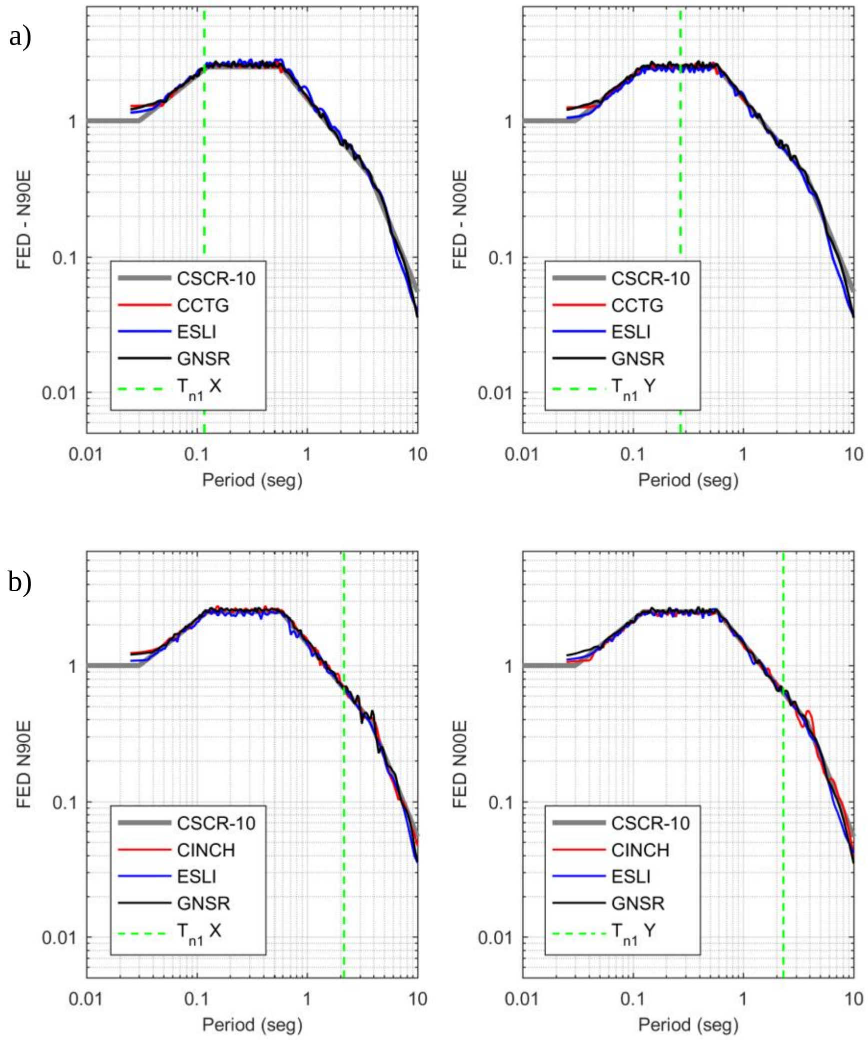

Figure 3. Response spectra of spectrally matched records in the two main direction of analysis for: a) RCM structure and b) DRC structure.

4. DAMAGE ANALYSIS

4.1 Nonlinear static analysis

The static pushover analysis has become a classical method also for vulnerability and expected damage and risk assessment of structures, due to its easy implementation and the fast and straightforward interpretation of results. Two disadvantages of this method lie in its dependency of the first mode behavior and in the independency of the structural behavior of several parameters of the seismic actions like duration, directionality, number of cycles with nonlinear incursion among others (Chandramohan, Baker, and Deierlein 2016; Vargas-Alzate et al. 2017).

Using the first mode as load pattern, the capacity curves were calculated in the two main directions of analysis for the two structures. Figure 4 shows the four capacity curves obtained for the two structures in the main directions of analysis. In the case of the RCM structure, both directions present a strong variation in the slope of the elastic branch (related with the period of the first mode), and the ultimate displacement. In both directions, the ultimate displacement ductility factor (defined as the relationship between the ultimate displacement and the yield displacement from the bilinear approximation) is similar.

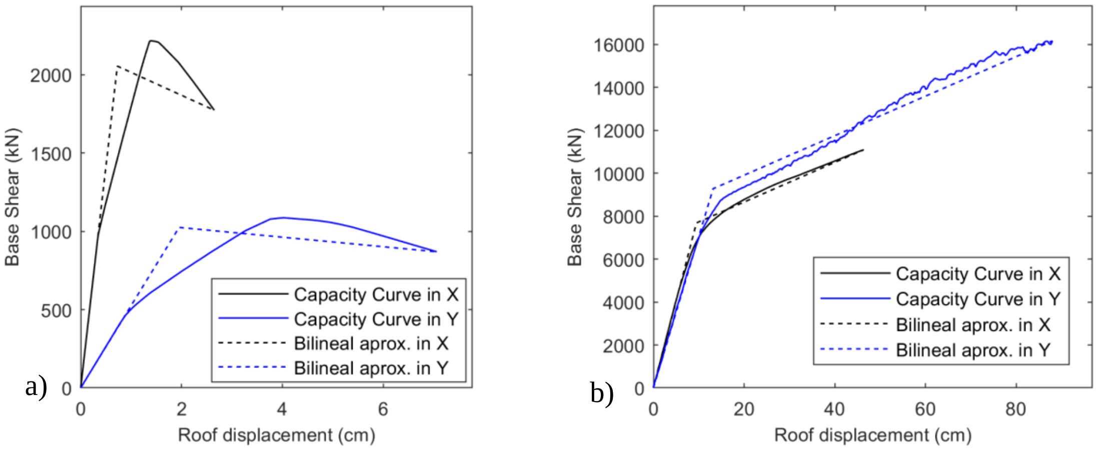

Figure 4. Capacity curves from a Pushover analysis for: a) RCM structure and b) DRC structure.

On the other hand, the DRC structure exhibits almost the same slope in the elastic section of the curve, but the ultimate ductility factors are not comparable. In a capacity spectrum analysis (Chopra and Goel 1999; Freeman 1998; Vargas-Alzate et al. 2013), the Y direction of the RCM structure will be the one that rules the damage in the structure, because it has a smaller base shear~~,~~ allowing the incursion into the nonlinear section for smaller acceleration values.

Meanwhile, in the DRC structure, the X direction is the weak direction, due to the smaller ultimate displacement and the similarity of the elastic section, so that one could expect an early collapse.

4.2 The Park and Ang Damage Index

The DI_{PA} (Park and Ang 1985), is a linear function of the maximum deformation and the effect of hysteretic loading. The employed parameters were calibrated with both monotonic and cyclic loading tests data. The damage index is defined as:

$$DI_{PA} = \frac{\mu_M}{\mu_u} + \frac{\beta}{F_y \mu_u \delta_y} \int dE \quad (1)$$

where μ_M is the maximum deformation ductility factor under earthquake, $\mu_u$is the ultimate (or maximum) ductility factor, β is a non-negative parameter taken as 0.05 (Carr 2003), dE is the energy differential in the hysteresis loop and δ_y and F_y are respectively the yielding displacement and strength.

Following the definition given in the original paper, DI_{PA} should have a value equal to zero (or negligibly small) under elastic response.

In this dynamic structural analysis, a three-dimensional model is used, so earthquakes are applied in the two main directions of the structure. Thus, the resultant damage index represents the overall damage to the structure after the dynamic load is applied.

4.3 Damage Index curves

Global structural damage, defined with the DI_{PA} damage index, is computed as the average of damage in every single element that presents damage (Carr 2003). Figure 5 shows damage curves obtained for both analyzed structures as a function of the Spectral Acceleration (Sa) at the period of the first mode. Given that there are two different values of Sa for each structure, one per each direction of analysis, and only one DI_{PA} value, an adjustment in the used Sa value was necessary.

As it can be observed in Figure 5, all the cases show a sudden increment in the value of DI_{PA}, from zero to approximately 0.15-0.3. This increment can be correlated with the first yield in the structure, and, even more, the first yield of a structural wall element. This kind of elements, in general, rules the nonlinear behavior of the structure due to their high contribution to the lateral load resistant system.

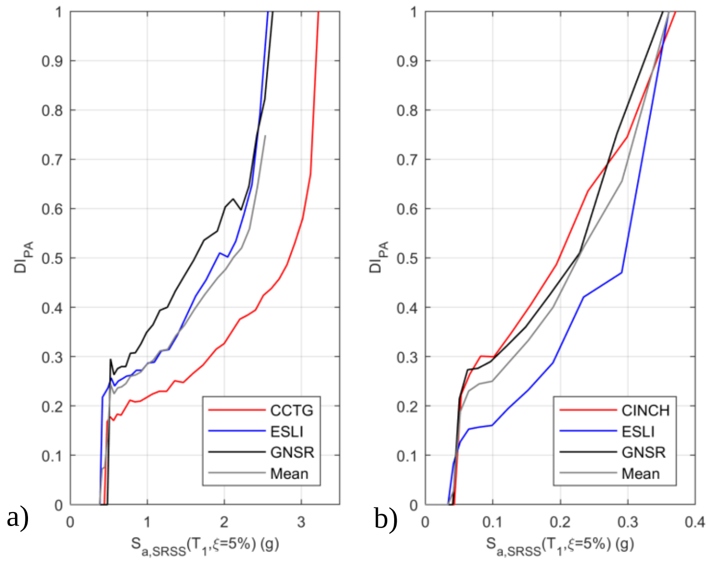

Figure 5. Variation of the DI_{PA} as a result of the IDA for: a) RCM structure and b) DRC structure.

Using the PGA defined for the design level of new structures located in the capital city of Costa Rica (PGA equal to 0.36g), and the corresponding elastic design spectrum for a soft soil (S_3 according with the CSCR-10 (CFIA 2011) and similar to D soil in ASCE 7-16 (ASCE 2017)), the corresponding design spectral accelerations for the first mode period are 0.9g for the RCM structure and 0.23g in the case of the DRC structure; in both cases, structures present mean damage indexes below 0.5 which can be related with a moderate damage state.

4.4 Simplified Damage Index from capacity curve

Given the high time consumption and complexity of IDA analysis, approximations bringing similar results but from simpler analyses are desirable. Pujades et al. (2015) proposed a simplified damage index equivalent to DI_{PA} which can be obtained from the capacity curve. This damage index follows the definition of the DI_{PA}, and is composed by two main sources: the energy dissipation $\left(E_N(\delta)\right)$ and the stiffness degradation $\left(K_N(\delta)\right)$, both defined as functions of the displacement in the capacity curve δ. The basic equations required to define the damage model are (Pujades et al. 2015):

$$E(\delta) = \int_0^{\delta} F_{NL}(\xi)d\xi\,; \quad 0 \le \delta \le \delta_u; \quad 0 \le E(\delta) \le E(\delta_u) \tag{2}$$

$$E_N(\delta_N) = \frac{E(\delta/\delta_u)}{E(\delta_u)}; \quad 0 \le \delta_N \le 1; \quad 0 \le E_N(\delta_N) \le 1 \tag{3}$$

$$K(\delta) = \frac{F(\delta)}{\delta} \tag{4}$$

$$K_{NL}(\delta) = \frac{\left[\frac{F(\delta)}{\delta}\right]_{max} - \frac{F(\delta)}{\delta}}{\left[\frac{F(\delta)}{\delta}\right]_{max} - \left[\frac{F(\delta)}{\delta}\right]_{min}}; \; 0 \le \delta \le \delta_u; \quad 0 \le K_{NL}(\delta) \le 1 \tag{5}$$

$$K_N(\delta_N) = K_{NL}(\delta/\delta_u); \; 0 \le \delta_N \le 1; \quad 0 \le K_N(\delta_N) \le 1 \tag{6}$$

$$DI_{CC}(\delta_N) = aK_N(\delta_N) + (1-a)E_N(\delta_N) \cong DI_{PA} \quad (7)$$

where F_{NL} is the nonlinear part of the capacity curve and has dimensions of force; δ and ξ are displacements from the capacity curve, δ_N is the displacement normalized at the ultimate displacement, E_N is the ratio between the energy dissipated as a function of the relative displacement, K_N is the ratio between the secant stiffness variation with respect to the maximum and a is a calibration non-negative parameter, related with the structural typology. This damage model has been applied with great results in reinforced concrete frames (Pujades et al. 2015) and steel special moment frames (Díaz et al. 2017).

Using the capacity curve for the weak direction in each structure (recall that the weak direction correlates with the global damage index) the DI_{CC} is calculated. Figure 6 shows the adjusted curves and the correspondent results from equations (3) and (6). The calibration constants used in this approximations are 0.891 for the RCM structure and 0.536 in DRC structure. In the calibration process, the mean DI_{PA} curve has been used. Damage is presented herein as a function of the displacement in the roof (in order to be consistent with the capacity curve), nevertheless, for comparison purposes, this curve will be presented as a function of an IM, like the spectral acceleration for the first mode period, as well.

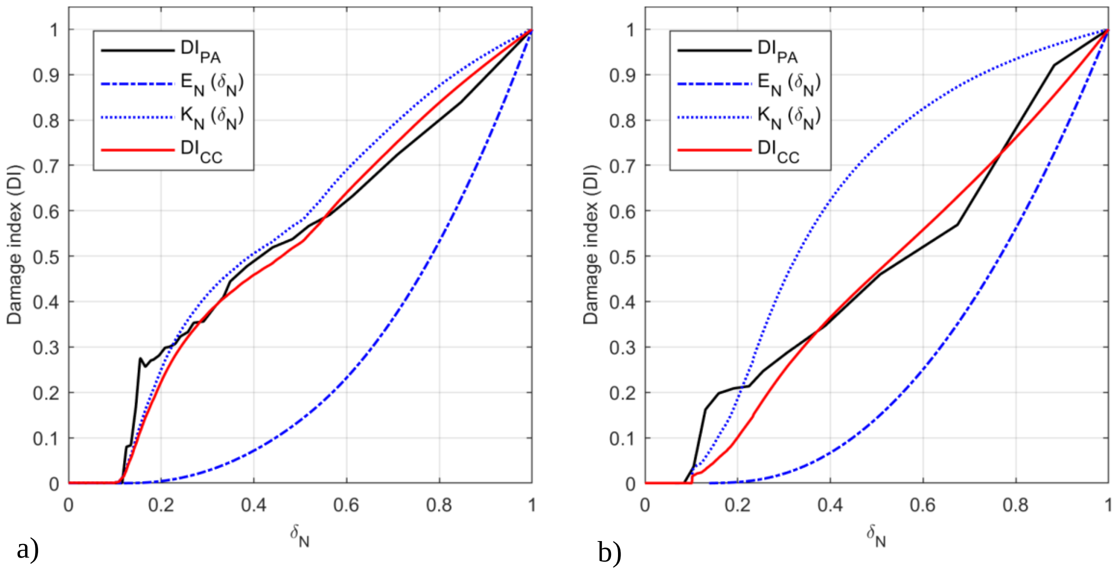

Figure 6. DI_{CC} defined from capacity curves for: a) RCM structure and b) DRC structure.

The resultant DI_{CC} curve shows a good agreement with the DI_{PA} curve which has been taken as target damage curve. The main differences are concentrated in the first yielding zone, where the DI_{PA} curve exhibits a sharp step of up to around 0.2. Thus, this simplified expedite Capacity curve based damage model brings results that are valid for global risk analysis, and from where one can also obtain fragility curves as a function of the roof displacement or any other IM. See Pujades et al. (2015) for details on how these fragility curves can be set up.

The RCM structure shows a stronger dependency on the wall elements, and as result, damage curves are more similar to the stiffness degradation curve, modelled with a high a constant. On the other hand, the DRC structure, present a mixed behavior, with a combination of both damage source curves, that is of the energy loss and stiffness degradation.

4.5 Improving the capacity-curve-based damage model

When the DI_{CC} was calculated for structures with a lateral load resistant system based on RC or steel frames (Díaz et al. 2017; Pujades et al. 2015), the obtained results were promising due to the excellent agreement with the DI_{PA} curve. These structures, are usually composed of high ductility elements, and therefore, the damage curve behavior is more like an "S" curve, like the ones shown in Figure 6. In these cases, the simplified damage index represents well the overall damage but fails to represent sharp damage increases.

Keeping that in mind, the first derivate of the capacity curve as a function of the displacement, represents the variation of tangent stiffness, and damage model of Pujades et al. (2015), can be modified by using the tangent stiffness degradation as a third damage source. The main advantage of using the tangent stiffness for brittle or semi-brittle structures is that the curve acquires the ability to represent well stepwise damage increases as the vertical variations in the DI_{PA} shown in Figure 6, which are attributed to the generation of plastic hinges, which are correlated with the structural damage. Thus, the tangent stiffness degradation function is defined as:

$$K_S(\delta) = m - \frac{d}{d\delta}F(\delta) \tag{8}$$

$$K_{SN}(\delta_N) = K_{TN}(\delta/\delta_u);\ 0 \le \delta \le \delta_u; \quad 0 \le K_{TN}(\delta) \le 1 \tag{9}$$

where m is the slope of the elastic section in the capacity curve and $F(\delta)$ is the capacity curve numerically defined as a function of the roof displacement. The improved damage model takes the following form:

$$DI_{ST}(\delta_N) = a\big(bK_N(\delta_N) + (1-b)K_S(\delta_N)\big) + (1-a)E_N(\delta_N) \tag{10}$$

where a and b are non-negative parameters, allowing to include the contribution to damage of the tangent stiffness degradation to the former damage simplified model. The a parameter measures the stiffness contribution in the damage model, meanwhile, the b parameter measures the relative contribution of the secant stiffness with respect to the tangent stiffness. Figure 7 shows the DI_{ST} and the functions of the three damage sources considered in the damage model.

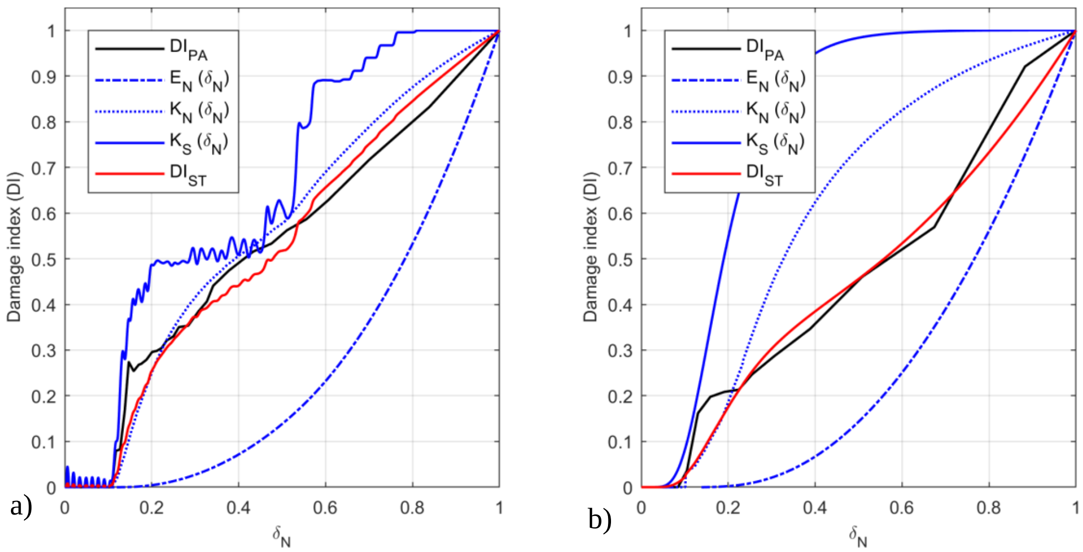

Figure 7. DI_{ST} defined from capacity curves for: a) RCM structure and b) DRC structure.

For the RCM structure, the fitting parameters are 0.85 and 0.79 for a and b respectively, while in the case of the DRC structure values of 0.431 and 0.466 were found respectively for a and b parameters.

Again, it can be seen the higher contribution of the stiffness degradation into the DI_{ST} damage model for the RCM structure, but in this case, with the addition of the tangent stiffness, the first stage of the damage curve, is slightly closer to the DI_{PA} damage curve. The same behavior occurs with the DRC structure but, in this case, the contribution of the energy accumulation is proportional to the stiffness degradation, so the impact of adding the tangent stiffness into the damage model is less marked.

4.6 Damage models comparison

In order to compare the two simplified damage models, a root-mean-squared error (RMSE) is calculated taking as target curve the original DI_{PA}. Table 3 shows the results obtained for the two damage models and the two analyzed structures. As can be seen, in both structures, the modified damage model (DI_{ST}) improve the fitting, resulting in a better characterization of the overall structural behavior.

Table 3. RMSE calculated between the original damage curve and the obtained with the simplified models.

Damage Model	**Structural model**	
	RCM	**DRC**
DI_{CC}	0.0323	0.0682
DI_{ST}	0.0275	0.0546

The use of the tangent stiffness degradation as damage parameters proves to be a valuable resource, catching some damage process hard to see with the other two damage sources employed in the DI_{CC}.

5. CONCLUSIONS

The Park and Ang damage model (1985) was successfully obtained for two different structures with high lateral flexural stiffness and a semi-brittle behavior. Also, two damage models obtained from the capacity spectrum have been also applied, obtaining a good agreement with the Park and Ang damage model, especially when the analysis was made considering the damage as a function of the roof displacement.

Both the simplified damage model and the improved version with the tangent stiffness, have proved to be a valid option for a fast structural damage assessment once the adjustment parameters have been defined. The inclusion of the tangent stiffness degradation improves in all the cases the approximation respects the original damage curve.

Damage evaluation according to the seismic code of Costa Rica (CFIA 2011), indicates a good behavior on the analyzed structures. Damage indexes are below the collapse and severe damage states, having an acceptable behavior according to the performance criteria defined in the same design code. Structures with semi-brittle elements and designed with an updated design code, as the one used in Costa Rica, shows a good behavior under seismic actions.

6. ACKNOWLEDGMENTS

This research was partially funded by the Ministry of Economy and Competitiveness (MINECO) of the Spanish Government and by the European Regional Development Fund (FEDER) of the European Union (UE) through projects referenced as: CGL2011-23621 and CGL2015-65913-P (MINECO/ FEDER, UE). The first author holds PhD fellowships from the OAICE, the Universidad de Costa Rica (UCR), and CONICIT, the Government of Costa Rica. Sergio Díaz also holds PhD fellowships from the Universidad Juárez Autónoma de Tabasco (UJAT) and from the PROMEP program. Finally, Luis A. Pinzón is supported by a Ph.D. scholarship grant from the "*Instituto para la Formación y Aprovechamiento de Recursos Humanos*" (IFARHU) and the "*Secretaría Nacional de Ciencias,* *Tecnología e Innovación*" (SENACYT) from the Government of Panama.

7. REFERENCES

ACI Committee 318. (2008). Building Code Requirements for Structural Concrete (ACI 318-08) and commentary (ACI 318R-08). American Concrete Institute, Farmington Hills, MI. https://doi.org/10.1016/0262-5075(85)90032-6

ASCE. (2017). Minimum Design Loads and Associated Criteria for Buildings and Other Structures (ASCE/SEI 7-16). American Society of Civil Engineers, Reston, VA. https://doi.org/10.1061/9780784414248

Bommer JJ, Bénito B, Ciudad-Real M, Lemoine A, López Menjívar M, Madariaga R, Rosa H (2010). The El Salvador earthquakes of January and February 2001 : context, characteristics and implications for seismic risk. *Soil Dynamics and Earthquake Engineering*, 22(5): 389–418. https://doi.org/10.1016/S0267-7261(02)00024-6

Carr A (2003). RUAUMOKO The Maori God of Volcanoes and Earthquakes. Volume 3: User Manual for the 3-Dimensional Version. Ruaumoko3D. University of Canterbury, Christchurch.

CFIA. (2011). Código Sísmico de Costa Rica 2010, 4th ed., Editorial Tecnológica de Costa Rica, Cartago, Costa Rica.

Chandramohan R, Baker JW, Deierlein GG (2016). Quantifying the influence of ground motion duration on structural collapse capacity using spectrally equivalent records. *Earthquake Spectra*, 32(2): 927–950. https://doi.org/10.1193/122813EQS298MR2

Chopra AK, Goel RK (1999). Capacity-demand-diagram methods based on inelastic design spectrum. *Earthquake Spectra*, 15(4): 637–655. https://doi.org/10.1193/1.1586065

D'Ayala D, Meslem A, Vamvatsikos D, Porter K, Rossetto T, Crowley H, Silva V (2014). Guidelines for analytical vulnerability assessment of low-to mid-rise buildings-Methodology, Vulnerability Global Component porject.

Díaz SA, Pujades LG, Barbat AH, Hidalgo-Leiva DA, Vargas-Alzate YF (2017). Capacity, damage and fragility models for steel buildings: a probabilistic approach. *Bulletin of Earthquake Engineering*, 16(3): 1209-1243. https://doi.org/10.1007/s10518-017-0237-0

Esquivel JC (1992). Influence of some parameters on the inelastic earthquake response using different histeretic models for reinforced concrete. *Proceedings of the 10th World Conference of Earthquake Engineering*. Rotterdam.

Freeman S (1998). The Capacity Spectrum Method as a Tool for Seismic Design. *Proceedings of the 11th European Conference on Earthquake Engineering*. Paris.

Giberson MF (1967). *The Response of Nonlinear Multi-story Structures Subjected to Earthquake Excitation*. California Institute of Technology, Pasadena, California.

Hancock J, Bommer JJ (2007). Using spectral matched records to explore the influence of strong-motion duration on inelastic structural response. *Soil Dynamics and Earthquake Engineering*, 27(4): 291–299. https://doi.org/10.1016/j.soildyn.2006.09.004

Hidalgo-Leiva DA (2017). Análisis estructural probabilista orientado a evaluación del daño sísmico con aplicaciones a tipologías constructivas empleadas en Costa Rica, *PhD Thesis,* Department of Civil and Environmental Engineering, Universitat Politècnica de Catalunya Barcelona Tech, Spain

Hidalgo-Leiva DA, Barbat AH, Pujades LG, Acuña D (2016). Experimental analysis of in-plane shear strength of reinforced concrete masonry wall and its seismic behavior. In: Modena C, da Porto F, Valluzzi M (eds.), Brick and Block Masonry: Trends, Innovations and Challenges - Proceedings of the 16th International Brick and Block Masonry Conference, IBMAC 2016, CRC, pp. 2295–2302. Padova, Italy.

Jacob KH, Pacheco J (1991). Seismology and Tectonics. *Earthquake Spectra*, 7(S2): 15–33.

Kingsley GR, Shing PB, Gangel T, NIST (2014). Seismic Design of Special Reinforced Masonry Shear Walls: A Guide for Practicing Engineers. Gaithersburg, MD.

Lagomarsino S, Penna A, Galasco A, Cattari S (2013). TREMURI program: An equivalent frame model for the nonlinear seismic analysis of masonry buildings. *Engineering Structures*, 56, 1787–1799. https://doi.org/10.1016/j.engstruct.2013.08.002

Linkimer L, Arroyo I, Mora MM, Vargas A, Soto G, Barquero R, Taylor M (2013). EL TERREMOTO DE SÁMARA (COSTA RICA) DEL 5 DE SETIEMBRE DEL 2012 (Mw 7.6). *Revista Geológica de América Central*, 49: 73–82.

Madan A, Reinhorn A, Mander JB, Valles RE (1997). Modeling of masonry infill panels for structural analysis. *Journal of Structural Engineering*, (October): 1295–1302.

Park Y, Ang A (1985). Mechanistic seismic damage model for reinforced concrete. *Journal of Structural Engineering*, Ill(4): 722–739.

Pujades LG, Vargas-Alzate YF, Barbat AH, González-Drigo JR (2015). Parametric model for capacity curves. *Bulletin of Earthquake Engineering*, 13(5): 1347–1376. https://doi.org/10.1007/s10518-014-9670-5

RSN (2009). El terremoto de Cinchona del jueves 8 de Enero de 2009. *Revista Geológica de América Central*, 40(1): 91–95.

Saidi M, Sozen M (1979). *Simple and complex models for nonlinear seismic response of reinforced concrete structures*. Structural Research Series. University of Illinois at Urbana-Champaign, Illinois.

Seible F, Priestley MJN, Kingsley GR, Kürkchübasche AG (1994). Seismic Response of Full-Scale Five-Story Reinforced-Masonry Building. *ASCE Journal of Structural Engineering*, 120(3): 925–946.

Vamvatsikos D, Cornell CA (2002). Incremental dynamic analysis. *Earthquake Engineering* and *Structural Dynamics*, 31(3): 491–514. https://doi.org/10.1002/eqe.141

Vargas-Alzate YF, Pujades LG, Barbat AH, Hurtado JE (2013). Capacity, fragility and damage in reinforced concrete buildings: a probabilistic approach. *Bulletin of Earthquake Engineering*, 11(6): 2007–2032. https://doi.org/10.1007/s10518-013-9468-x

Vargas-Alzate YF, Pujades LG, Barbat AH, Hurtado JE, Diaz SA, Hidalgo-Leiva DA (2017). Probabilistic seismic damage assessment of reinforced concrete buildings considering direccionality effects. *Structure and Infrastructure Engineering*, (October): 1–13. https://doi.org/10.1080/15732479.2017.1385089